

1 **Analyzing and Visualizing Ancient Maya Hieroglyphics Using Shape:** 2 **from Computer Vision to Digital Humanities**

3 Rui Hu

4 Idiap Research Institute, Switzerland

5 Carlos Pallán Gayol

6 University of Bonn, Germany

7 Jean-Marc Odobez

8 Idiap Research Institute

9 École Polytechnique Fédérale de Lausanne (EPFL), Switzerland

10 Daniel Gatica-Perez

11 Idiap Research Institute

12 École Polytechnique Fédérale de Lausanne (EPFL), Switzerland

13 **Abstract**

14 Maya hieroglyphic analysis requires epigraphers to spend a significant amount of time browsing
15 existing catalogs to identify individual glyphs. Automatic Maya glyph analysis provides an
16 efficient way to assist scholars' daily work. We introduce the Histogram of Orientation Shape
17 Context (HOOSC) shape descriptor to the digital humanities community. We discuss key issues
18 for practitioners and study the effect that certain parameters have on the performance of the
19 descriptor. Different HOOSC parameters are tested in an automatic ancient Maya hieroglyph
20 retrieval system with two different settings, namely when shape alone is considered and when
21 glyph co-occurrence information is incorporated. Additionally, we developed a graph-based
22 glyph visualization interface to facilitate efficient exploration and analysis of hieroglyphs.
23 Specifically, a force-directed graph prototype is applied to visualize Maya glyphs based on their
24 visual similarity. Each node in the graph represents a glyph image; the width of an edge
25 indicates the visual similarity between the two according glyphs. The HOOSC descriptor is used
26 to represent glyph shape, based on which pairwise glyph similarity scores are computed. In
27 order to evaluate our tool, we designed evaluation tasks and questionnaires for two separate
28 user groups, namely a general public user group and an epigrapher scholar group. Evaluation
29 results and feedback from both groups show that our tool provides intuitive access to explore
30 and discover the Maya hieroglyphic writing, and could potentially facilitate epigraphy work. The

31 positive evaluation results and feedback further hints the practical value of the HOOSC
32 descriptor.

33 **1. Introduction**

34 Technological advances in digitization, automatic image analysis, and information management
35 are enabling the possibility to analyze, organize and visualize large cultural datasets. As one of
36 the key visual cues, shape has been used in various image analysis tasks such as handwritten
37 character recognition (Fischer et al., 2012; Franken et al., 2013), and sketch analysis (Eitz et al.,
38 2012). We assess a shape descriptor, within the application domain of Maya hieroglyphic
39 analysis. Our aim is to introduce this descriptor to the wider Digital Humanities (DH) community,
40 as a shape analysis tool for DH-related applications. Two example application systems, namely
41 an automatic glyph retrieval framework and an interactive glyph visualization interface are
42 presented.

43 The Maya civilization is one of the major cultural developments in ancient Mesoamerica. The
44 ancient Maya language created uniquely pictorial forms of hieroglyphic writing (Stone et al.,
45 2011). Most Maya texts were written during the Classic period (AD 250-900) of the Maya
46 civilization on various media types, including stone monuments, architectural elements, as well
47 as personal items. A special class of Maya texts was written on bark cloths, made from the inner
48 bark of certain trees (the main being the ficus tree), as folding books from the Post-Classic
49 period (AD 1000-1519). Only three such books (namely the Dresden, Madrid and Paris codices)
50 are known to have survived the Spanish Conquest. A typical Maya codex page contains icons,
51 main sign glyph blocks, captions, calendric signs, etc. In this paper, we are interested in the
52 main signs.

53 Maya hieroglyphic analysis requires epigraphers to spend a significant amount of time browsing
54 existing catalogs to identify individual glyphs. Automatic Maya glyph analysis provides a
55 potentially efficient way to assist scholars' daily work. Identifying unknown hieroglyphs can be
56 addressed as a shape matching problem. A robust shape descriptor called Histogram of
57 Orientation Shape Context (HOOSC) was developed in (Roman-Rangel et al., 2011). Since
58 then, HOOSC has been successfully applied for automatic analysis of other cultural heritage
59 data, such as Oracle-Bones Inscriptions of ancient Chinese characters (Roman-Rangel, 2012),
60 and ancient Egyptian hieroglyphs (Franken et al., 2013). It has also been applied for generic
61 sketch and shape image retrieval (Roman-Rangel, 2012). Our recent work extracted a statistic
62 Maya language model and incorporated it for glyph retrieval (Hu et al., 2015).

63 In another direction, data visualization techniques, which organize and present data in a
64 structured graphical format, can be applied to visualize glyph images, enable efficient browsing
65 and search of ancient hieroglyph datasets. Such systems can enable mining and discovery of
66 visual and semantic patterns of the ancient Maya writing, which could potentially facilitate
67 research aimed at advancing hieroglyphic decipherment. We developed an interactive, graph-
68 based glyph visualization interface.

69 In this paper, we introduce the HOOSC descriptor to the digital humanities community. We
70 discuss key issues for practitioners and study the effect that certain parameters have on the
71 performance of the descriptor. Different HOOSC parameters are tested in an automatic ancient
72 Maya hieroglyph retrieval system with two different settings, namely when shape alone is
73 considered and when glyph co-occurrence information is incorporated. Additionally, we present
74 a graph-based visualization interface, where each node in the graph represents a glyph image,
75 an edge between two nodes indicate the visual similarity of the two corresponding glyphs. Glyph
76 visual similarity measurement is an important factor which affects the layout of the graph. In this
77 paper, the HOOSC descriptor was used to represent the shape of each glyph, based on which
78 glyph visual similarity scores were computed. Our interface was developed using the force
79 directed graph prototype of the D3 (Data-Driven Document) web-based visualization approach
80 (Bostock et al., 2011).

81 The goal of this paper is three-fold:

- 82 1. Introduce the HOOSC descriptor to be used in DH-related shape analysis tasks (code
83 available at: <http://www.idiap.ch/project/maaya/code/>);
- 84 2. Discuss key issues for practitioners, namely the effect that certain parameters have on
85 the performance of the descriptor. We describe the impact of such choices on different
86 data types, specially for 'noisy' data as it is often the case with DH image sources;
- 87 3. Present and evaluate a graph-based, glyph visualization interface to explore Maya
88 hieroglyph data. The HOOSC descriptor is applied to represent the shape feature of
89 glyph images, based on which pairwise glyph visual similarity scores are computed to
90 define the edges in the graph.

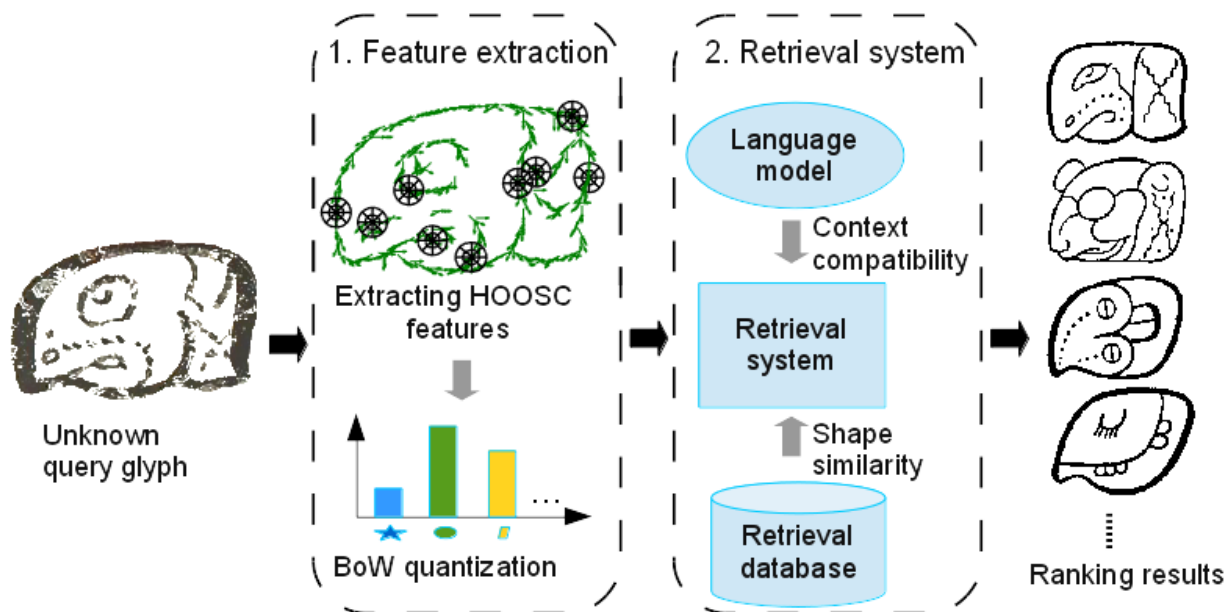
91 A preliminary version of this paper was presented in the Digital Humanities conference (Hu et
92 al., 2016).

93 The rest of the paper is organized as follows: In section 2, we introduce the HOOSC descriptor
94 and discuss the key issues of certain parameters have on the performance of the descriptor in a

95 state-of-the-art glyph retrieval system; in section 3, we present a graph-based interactive glyph
96 visualization interface, where the HOOSC descriptor is used to represent the shape of glyph
97 images; we draw concluding remarks in section 4.

98 2. Automatic Maya Hieroglyph Recognition

99 We conduct glyph recognition with a retrieval system proposed in (Hu et al., 2015). Unknown
100 glyphs are considered as queries to match with a database of known glyphs (retrieval database).
101 Shape and context information are considered. Fig. 1 illustrates a schema of our approach. We
102 study the effect of different HOOSC parameter choices on the retrieval results.



103

104 *Fig. 1 Retrieval system pipeline.*

105 2.1 Datasets


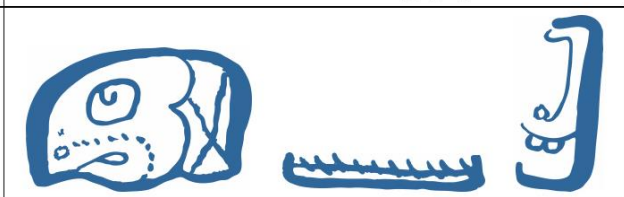



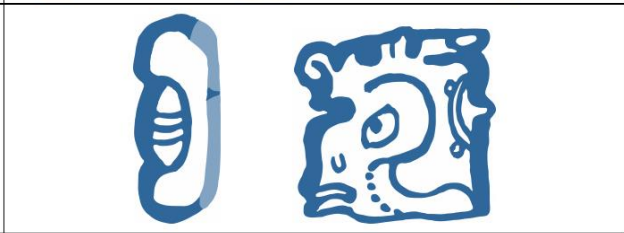
106 We use three datasets, namely the 'Codex', 'Monument' and 'Thompson'. The first two are used
107 as queries to search within the retrieval database ('Thompson').



108




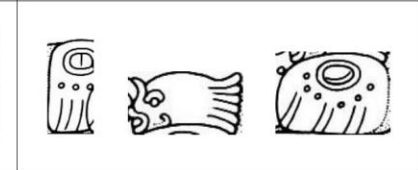

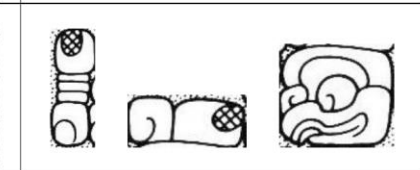
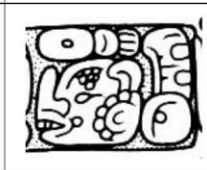
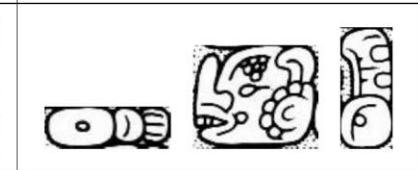
109 *Fig. 2 Digitization quality: (left) raw glyph blocks cropped from Dresden codex; (middle) clean*
 110 *raster images produced by removing the background noise; (right) reconstructed high-quality*
 111 *vectorial images.*

112 The 'Codex' dataset contains glyph blocks from the three surviving Maya codices. Fig. 2 shows
 113 examples of three raw glyph block images cropped from the ancient codices (Fig. 2 left); their
 114 clean raster versions (Fig. 2 middle); and high-quality reconstructed vectorial images (Fig. 2
 115 right). Clean raster and reconstructed versions are manually generated by epigraphers in our
 116 team. The clean raster images are produced by manually removing the background area from
 117 the raw images; whereas the reconstructed forms are generated by further carefully
 118 reconstructing the broken lines and missing strokes. Glyph blocks are typically composed of
 119 combinations of individual signs. Fig. 3 shows individual glyphs segmented from blocks in Fig. 2.
 120 Note the different degradation levels across samples. We use two sub-datasets: 'codex-small',
 121 composed of 156 glyphs segmented from 66 blocks, for which we have both clean raster and
 122 high-quality reconstructed vectorial representations (see Fig. 3) to study the impact of the
 123 different data qualities on the descriptor; and a 'codex-large' dataset, which is more extensive,
 124 comprising only the raster representation of 600 glyphs from 229 blocks.

Clean raster	Reconstructed glyphs
	
	
	

125
126 *Fig. 3 Example glyph strings generated from blocks shown in Figure 2.*

127 The 'Monument' dataset is an adapted version of the Syllabic Maya dataset used in (Roman-
128 Rangel et al., 2011), which contains 127 glyphs of 40 blocks extracted from stone monuments. It
129 is a quite different data source to the codex data, in terms of historical period, media type, and
130 data generation process. Samples are shown in Fig. 4.

Block	Segmented glyphs	Block	Segmented glyphs
			
			

131
132 *Fig. 4 Example blocks and segmented glyph strings form the 'Monument' dataset.*

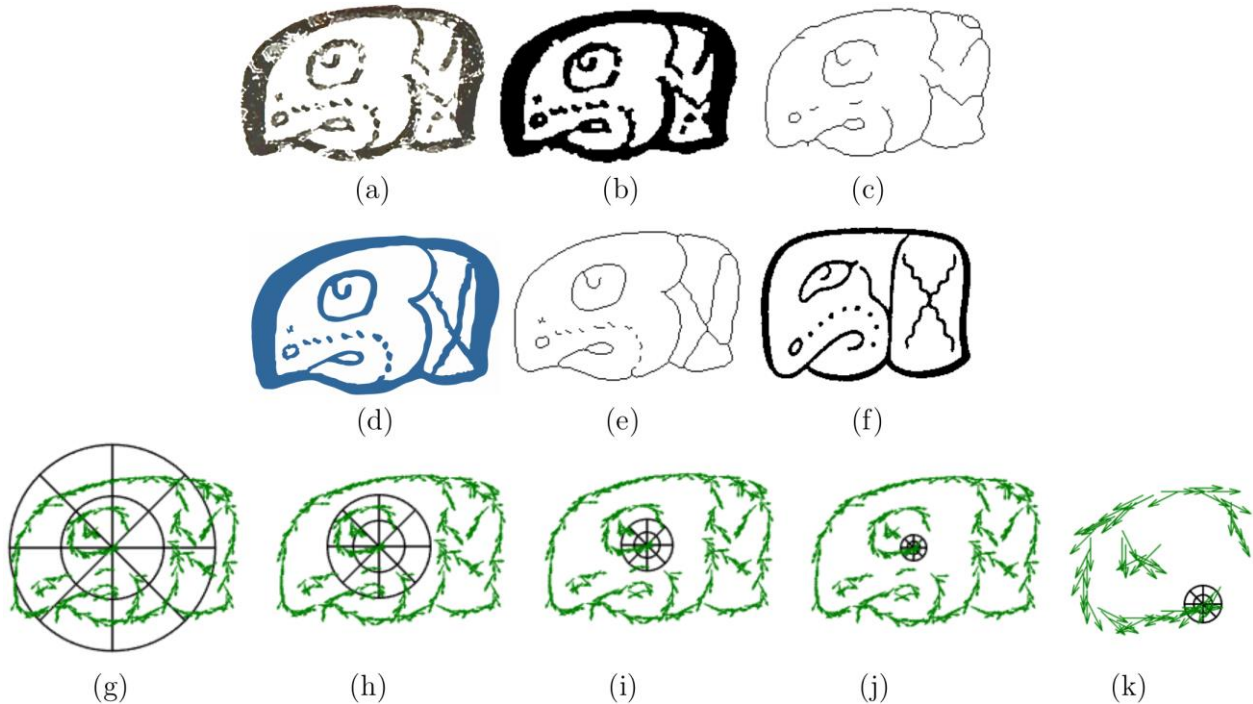
133 To form the retrieval database ('Thompson'), we scanned and segmented all the glyphs from the
134 Thompson catalog (Thompson, 1962). The database contains 1487 glyph examples of 892
135 different sign categories. Each category is usually represented by a single example image.
136 Sometimes multiple examples are included; each illustrates a different visual instance or a
137 rotation variant. Fig. 5 shows glyph examples.

T0501	T0502	T0668	T0757	T0102	T0103
/b'a/	/ma/	/cha/	/b'a/	/ki/	/ta/

138
139 *Fig. 5 Thompson numbers, visual examples, and the syllabic values of glyph pairs. Each pair*
140 *contains two different signs with similar visual features (Hu et al., 2015). All examples are taken*
141 *from (Thompson, 1962).*

142 **2.2 Shape-based retrieval**

143 Feature extraction and similarity matching are the two main steps for our shape-based glyph
144 retrieval framework.



145
146 *Fig. 6 Extracting HOOSC descriptor: (a) input clean raster image; (b) binary image; (c) thinned*
147 *edge of (b); (d) reconstructed vector representation of (a); (e) thinned edge of (d); (f)*
148 *corresponding groundtruth image in the catalog; (g)-(k) spatial partition of a same pivot point*
149 *with five different ring sizes (1, $\frac{1}{2}$, $\frac{1}{4}$, $\frac{1}{8}$, $\frac{1}{16}$, all defined as a proportion to the mean of the*
150 *pairwise distance between pivot points) on the local orientation field of the thinned edge image*
151 *(c). Note that we zoomed in to show the spatial context of 1/16 in (k).*

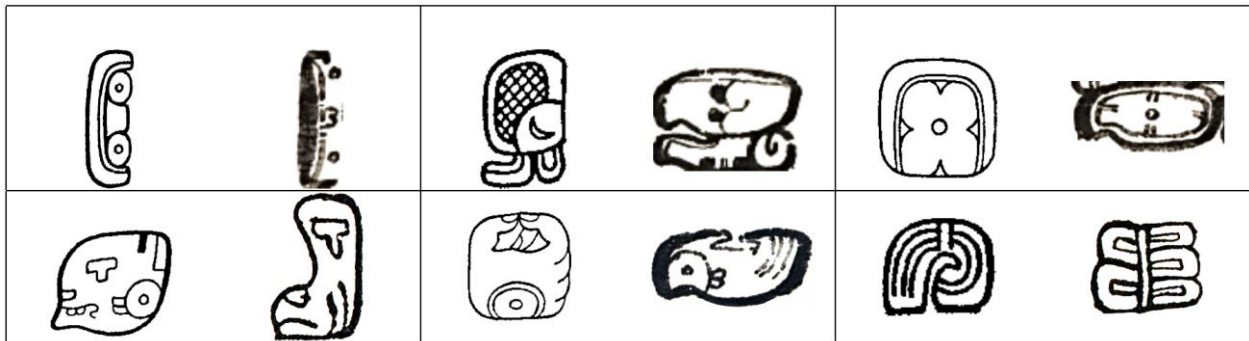
152 Glyphs are first pre-processed into thin lines. To do so, an input glyph (Fig. 6(a)) is first
153 converted into a binary shape (Fig. 6 (b)). Thin lines (Fig. 6(c)) are then extracted through

154 mathematical morphology operations. Fig. 6(d)-(e) show the high-quality reconstructed binary
155 image and the extracted thin lines.

156 HOOSC descriptors are then computed at a subset of uniformly sampled pivot points along the
157 thin lines. HOOSC combines the strength of Histogram of Orientation Gradient (Dalal et al.,
158 2005) with circular split binning from the shape context descriptor (Belongie et al., 2002). Given
159 a pivot point, the HOOSC is computed on a local circular space centred at the pivot's location,
160 partitioned into rings and evenly distributed angles. Fig. 6 (g)-(k) show different sizes of the
161 circular space (referred to as spatial context) partitioned into 2 rings and 8 orientations. A
162 Histogram-of-orientation-gradient is calculated within each region. The HOOSC descriptor for a
163 given pivot is the concatenation of histograms of all partitioned regions.

164 We then follow the Bag-of-Words (BoW) approach, where descriptors are quantized as visual
165 words based on the vocabulary obtained through K-means clustering on the set of descriptors
166 extracted from the retrieval database. A histogram representing the count of each visual word is
167 then computed as a global descriptor for each glyph. In all experiments, we use vocabulary size
168 $k=5000$.

169 Each query is matched with glyphs in the retrieval database, by computing shape feature
170 similarity using the L1 norm distance.



171
172 *Fig. 7 Six pairs of glyph signs (Hu et al., 2015). Each pair contains a query glyph from the*
173 *'Codex' dataset (right) and their corresponding groundtruth in the catalog (left).*

174 **2.3 Incorporating context information**

175 Shape alone is often ambiguous to represent and distinguish between images. In the case of our
176 data, different signs often share similar visual features (see Fig. 5); glyphs of the same sign
177 category vary with time, location, and the different artists who produced them (see Fig. 7);

178 additionally, surviving historical scripts often lose visual quality over time. Context information
179 can be used to complement the visual features.

180 Glyph co-occurrence within single blocks encodes valuable context information. To utilize this
181 information, we arrange glyphs within a single block into a linear string according to the reading
182 order (see Fig. 3 and Fig. 4) and consider the co-occurrence of neighbouring glyphs using an
183 analogy to a statistical language model. For each unknown glyph in the string, we compute its
184 probability to be labelled as a given category by considering not only the shape similarity, but
185 also the compatibility to the rest of the string.

186 We apply the two glyph co-occurrence models (statistic language models) extracted in (Hu et al.,
187 2015), namely the ones derived from the Maya Codices Database (Vail et al., 2013) and the
188 Thompson catalog (Thompson, 1962), which we refer to as the 'Vail' and the 'Thompson'
189 models. We use Vail model with smoothing factor $\alpha=0$ for the 'Codex' data, and the Thompson
190 model with $\alpha=0.2$ for the 'Monument' data, which have shown to perform well in (Hu et al., 2015).

191 **2.4 Experiments and Results**

192 Our aim is to demonstrate the effect of various HOOSC parameters on retrieval results.

193 **2.4.1 Experimental setting**

194 We illustrate the effect of 3 key parameters:

- 195 • Size of the spatial context region within which HOOSC is computed

196 A larger region encodes more context information and therefore captures more global structure
197 of the shape. However, in the case of image degradation, a larger region could contain more
198 noise. We evaluate five different spatial contexts as shown in Fig. 6(g)-(k). The circular space is
199 distributed over 8 angular intervals.

- 200 • Number of rings to partition the local circular region

201 This parameter represents different partition details. We evaluate either 1 or 2 rings, the inner
202 ring covers half the distance to the outer ring. Each region is further characterized by a 8-bin
203 histogram of the local orientations.

- 204 • Position information

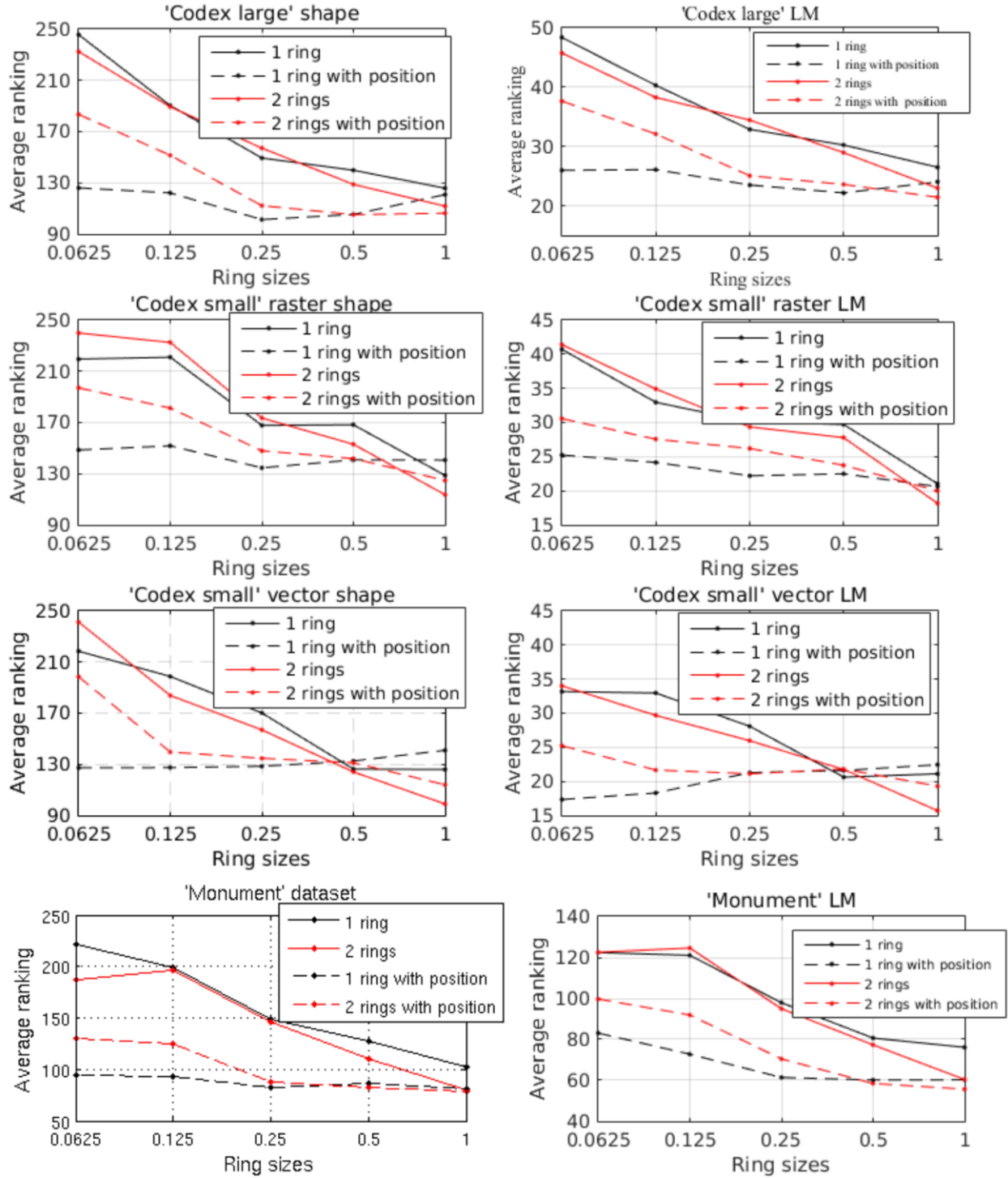
205 Relative position (i, j) of a pivot in the 2-D image plane can be concatenated to the
206 corresponding HOOSC feature.

207 **2.4.2 Results and discussion**

208 Fig. 8 shows the average groundtruth ranking in the retrieval results with different parameter
209 settings, on three query sets, *e.g.* 'Codex-large', 'Codex-small' and 'Monument'. Each query
210 image usually has only one correct match (groundtruth) in the retrieval database. The smaller
211 the average ranking value, the better the result. From Fig. 8 we can see the following:

- 212 • In most cases, the best results are achieved by using the largest spatial context, with
213 finer partitioning details (2 rings in our case);
- 214 • When the location information is not considered, results show a general trend of
215 improving with increasing ring sizes. However, the results are more stable when the
216 position information is encoded, *e.g.* a smaller ring size can also achieve promising
217 results when the location information is incorporated. This is particularly useful when
218 dealing with noisy data, where a smaller ring size is preferred to avoid extra noise been
219 introduced by a larger spatial context;
- 220 • The results do not benefit from a finer partition when a small spatial context is
221 considered. However, results improve with finer partitions when the spatial context
222 becomes larger.
- 223 • Position information is more helpful when a small spatial context is considered.

224 Fig. 9 shows example query glyphs and their top returned results.



225
 226 *Fig. 8 Retrieval results on each dataset, with various feature representation choices. (left) shape-*
 227 *base results; (right) incorporating glyph co-occurrence information.*



228
229
230

Fig. 9 Example queries (first column) and their top returned retrieval results, ranked from left to right in each row. Groundtruth images are highlighted in green bounding boxes.

231 **3. Graph-based Glyph Visualization Interface**

232 We developed a web-based visualization interface to enable efficient exploration of ancient
233 Maya hieroglyph signs. Our tool can not only be used by general public users to browse and
234 explore the ancient Maya hieroglyph writing system, but also by epigraphy scholars as a tool to
235 facilitate their daily work of glyph analysis, as well as to discover visual and semantic glyph
236 patterns.

237 In this section, we first explain the methodology that we followed to develop this tool and its
238 functionalities; we then present our evaluation tasks, together with the evaluation results and
239 feedback collected from both general users and epigraphy expert users.

240 ***3.1 Visualization approach***

241 Maya hieroglyph sign examples, scanned and segmented from the Thompson catalog
242 (Thompson, 1962), are illustrated in a force-directed graph. Each node in the graph corresponds
243 to one glyph image in the database. The width of an edge indicates the visual similarity score
244 between the two corresponding glyphs. A detailed explanation of how to compute the glyph
245 similarity scores, and the specific design and functionalities of our tool are introduced below.

246 **3.1.1 Glyph visual similarity measurement**

247 Visual similarity is an important factor which defines the layout of the graph, and therefore
248 affects the performance of the visualization tool. We use the HOOSC descriptor to represent
249 glyph shape, based on which the visual similarity scores are computed.

250 Given the glyph sign examples in the Thompson catalog, we focus on the signs that appear in
251 the three surviving ancient Maya codices. Based on our annotation of the Maya codex database,
252 there are in total 288 different glyph sign categories appeared in the three codices, which
253 corresponds to 657 image examples in the Thompson catalog. Each of these images defines a
254 node in the graph.

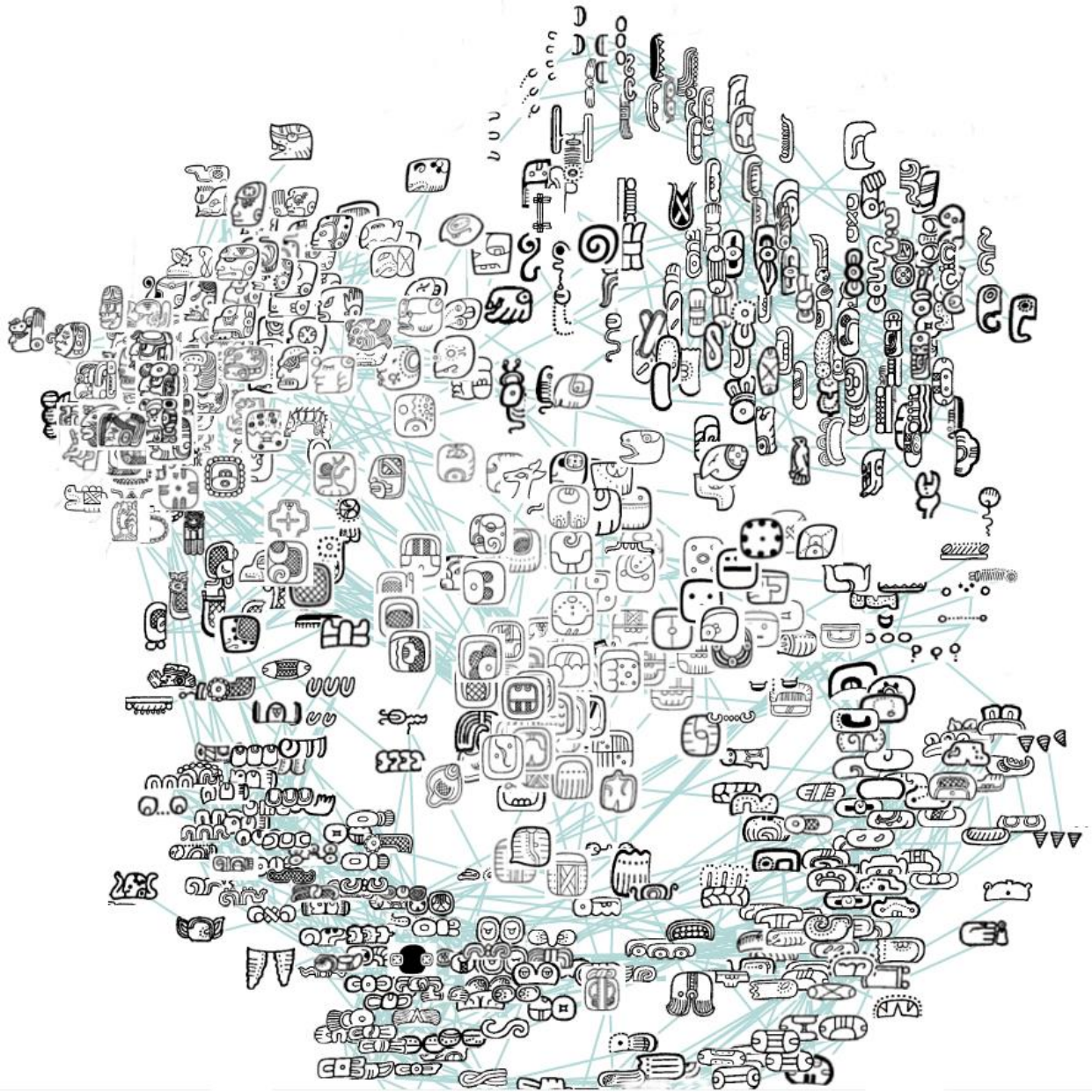
255 Following the framework introduced in section 2.2, we first extract the HOOSC descriptors for
256 each image and then compute glyph similarity scores between image pairs. Specifically, we
257 conduct the following process. First, each glyph image is pre-processed into thin lines; 400
258 evenly distributed points along the lines are randomly selected as pivot points. The HOOSC
259 descriptor for each pivot point is then computed on a circular region centered at the pivot
260 location, with a diameter equal to the mean of the pairwise distance between pivot points, which
261 is partitioned into 2 rings and 8 equally distributed orientations. The bag of words pipeline, with

262 vocabulary size $k=5000$, is then applied to compute a global histogram representation indicating
263 the count of each visual word. Finally, the pairwise glyph visual similarity is computed based on
264 the L1 norm distance measure.

265 The resulted graph has 657 nodes and 215496 edges. In order to reduce the complexity of the
266 graph, we reduced the number of edges by applying a threshold to the similarity scores. Two
267 glyph images are only considered to be similar if their visual similarity score is larger than a pre-
268 defined threshold α , and therefore their corresponding nodes in the graph are connected.
269 Otherwise, the two glyphs are not considered to be sufficiently similar, and their corresponding
270 nodes in the graph are not connected. A higher threshold indicates that fewer glyph pairs are
271 considered to be visually similar, which results in fewer edges in the graph. In contrast, a smaller
272 threshold indicates that more glyph pairs are considered to be visually similar, which leads to a
273 more connected graph (more edges). In this paper, we take the threshold $\alpha=0.2$ as an example
274 for user evaluation tasks in the following sections. The reduced graph has 687 edges.
275 Visualization graph with different threshold scores can be explored at: <http://lab.idiap.ch/maaya/>.

276 **3.1.2 Design and functionality**

277 We use the force-directed graph layout provided in the D3 visualization approach. D3 is a web-
278 based, representation-transparent visualization approach. Given a glyph image database, we
279 initialize the graph with random node positions and the pre-computed pairwise glyph similarity
280 scores as edge weights. The force-directed graph optimizes to position nodes of the graph so
281 that there are as few crossing edges as possible, and all the edges are of roughly similar length.
282 As a result, nodes in the graph often fall in several groups, each containing glyphs of visually
283 similar patterns. Fig. 10 illustrates our visualization interface. It can be seen that glyphs are
284 grouped into visually similar clusters, such as vertical, horizontal, squared, and knot shaped
285 patterns. This could naturally function as a shape-based glyph indexing system, which could
286 help users quickly identify an unknown glyph based on its visual features.



287

288 *Fig. 10 Graph-based visualization interface.*

289 We adapt a similar design to the 'movie network' example in D3¹. Our visualization tool allows
290 zooming, dragging, and clicking actions to facilitate exploring and analysis of the glyph
291 database. Upon clicking on a node, an information panel pops up. It shows the example image
292 of the corresponding node in the graph and more detailed information of the individual glyph.

293 Fig. 11 shows the pop up information panel of an example glyph. Three types of information are

¹ Movie network example: <http://bl.ocks.org/paulovn/9686202>

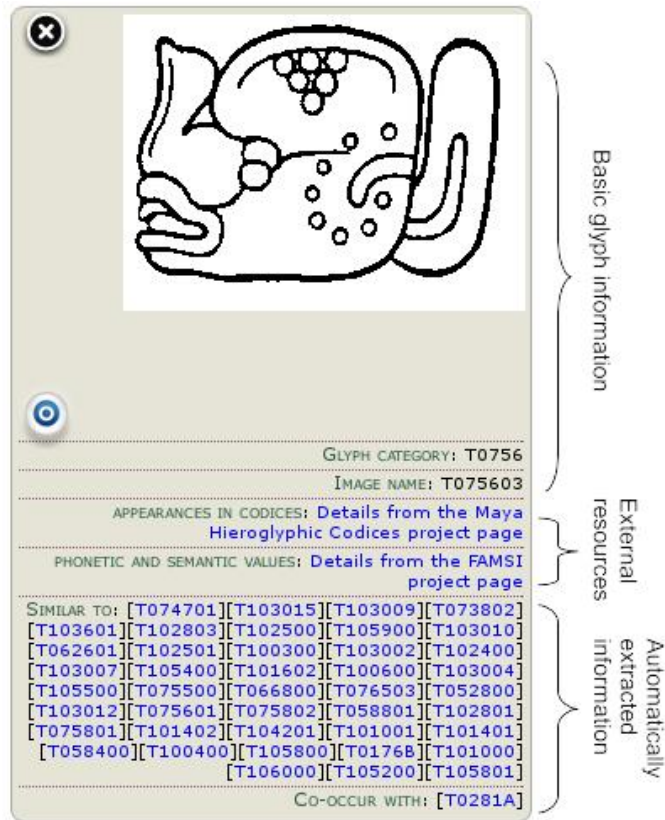
294 included in the panel. The first type shows the basic glyph information, which includes the glyph
295 example image shown at the top of the panel, the Thompson code ('Glyph category'), and the
296 index of this glyph variant ('Image name'). The second type provides information about external
297 resources, including the glyphs' 'Appearance in codices' and 'Phonetic and semantic values'.
298 Finally, the third type presents information that is automatically extracted from images based on
299 shape analysis ('Similar to') and the statistic glyph co-occurrence information ('Co-occur with')
300 extracted from the three surviving ancient Maya codices. Below, we give detailed explanation of
301 the latter two types of information shown in the pop up window.

302 **Links to external resources.**

303 By clicking on glyphs in the list of 'Appearance in codices', our interface leads users to an online
304 database provided by the Maya codices database project (Vail et al., 2013), where users can
305 browse through all the codex 'frames' from the three ancient codices in which this glyph appears.

306 By clicking on glyphs in the list of 'Phonetic and semantic values', the interface conducts users to
307 the John Montgomery Dictionary of Maya Hieroglyphs (Montgomery et al., 2007) via the
308 Foundation for the Advancement of Mesoamerican Studies, Inc. (FAMSI) webpage
309 (<http://www.famsi.org/>), which gives more detailed information of the given glyph, including its
310 pronunciation and semantic meaning if applicable, decoded by epigraphers over the years.

311 These functions provide users with access to valuable and already existing Maya hieroglyphic
312 resources, which can be used to facilitate scholars' work, and also to help members of the
313 general public interested in exploring the ancient Maya scripts. Our interface here serves as a
314 connecting point to richer resources.



315

316 *Fig. 11 Pop up information panel of an example glyph, upon clicking on the according node in*
 317 *the graph.*

318 **Automatically extracted information.**

319 Additionally, those glyphs that are considered to be visually similar to the current glyph are listed
 320 in the pop up information panel (following the 'Similar to' icon). This is automatically
 321 recommended based on the methodology presented in section 3.1.1. Glyphs shown from top to
 322 bottom, left to right in the list are ordered starting from the most similar one. Clicking on any
 323 glyphs in this list will launch an additional pop up information window of the according glyph.
 324 Browsing through similar glyphs in the list, users have an opportunity to further explore visually
 325 similar glyph patterns.

326 Last but not least, the statistical glyph co-occurrence information extracted from the three
 327 ancient codices is also listed in the information panel (following the 'Co-occur with' icon). The list
 328 is ordered from the highest to the lowest frequently co-occurring glyphs to the current glyph. The
 329 co-occurrence information provides users an opportunity to explore glyphs in a semantic level by
 330 considering the context information. This feature could be particularly useful to help understand
 331 problematic glyphs that are difficult to be identified using shape features alone.

332 **3.2 User evaluation**

333 We designed three user evaluation tasks to assess our tool. Our objectives are three-fold. First,
334 to evaluate whether our visualization interface can help users identify unknown glyphs efficiently.
335 Second, to understand whether the automatically recommended visually similar glyphs shown in
336 the information panel indeed share sufficiently similar visual features to the query glyph. Third, to
337 test whether the glyph co-occurrence information provided in the pop up information panel can
338 enable users to identify problematic glyphs by considering the context information within a block.
339 Additionally, we designed questionnaires to collect user feedback to improve our tool.

340 Two different user groups, namely a general public user group and an epigrapher scholar group,
341 were considered for the evaluation. The general public user group includes participants who
342 have never studied Maya hieroglyphs. For this experiment, we take advantage of two open door
343 exhibition events, one is at Idiap Research Institute and the other at EPFL. These events aim to
344 demonstrate scientific research to the local audience. We set our system in the context of these
345 exhibitions. The audience who participated in these events were from different backgrounds, and
346 their age ranged from around 5 to 70 years old. Once someone from the audience approached
347 our exhibition, we first briefly introduced the Maya culture and hieroglyphs, followed by a general
348 presentation of our project; we then introduce the functionality of our visualization interface.
349 Audiences who were further interested to try our interface, were invited to voluntarily participate
350 in our evaluation task. Within around 8 hours of total exhibition time for each event, there were
351 26 and 20 volunteers who participated in each study, respectively.

352 The epigrapher scholar group was formed by experienced Maya epigraphy scholar volunteers.
353 For this user group, we prepared a document which gave detailed explanation of the
354 functionality of our interface, and the designed tasks, followed with a questionnaire. We sent this
355 document via email to scholars possibly interested to test our tool. The evaluation process was
356 carried out by individual scholars independently without any supervision. We collected
357 evaluation results and feedback from three scholars. One of them reported to have less than 3
358 years' experience, and the other two scholars have 6-10 years' experience in research on Maya
359 hieroglyphs.

360 **3.2.1 Task I: Identifying unknown glyphs**

361 The first task aimed to assess whether our tool can assist users to identify an unknown glyph
362 efficiently, by searching the catalog glyphs visualized in the graph. Participants were advised to
363 use the shape cluster patterns shown in the graph as a way to reduce the searching space.

364 Given a query glyph, users first identify a particular shape group in the graph, which this query
365 glyph belongs to based on visual similarity; and then zoom in that particular group to search for
366 the exact match of the query glyph.

367 For this task, our study targeted both the general public and epigrapher scholars. The evaluation
368 criteria is the amount of time that users spent to find each query glyph.

369 **General public users.**

370 For the general public users, we selected 5 simple query glyphs, each representing a different
371 shape pattern (see Fig. 12). Users were advised to pick any glyph(s) to work with.

372 From the returned results, we observed that most users tried to search for only one glyph, while
373 some tried to search for more. There were in total 81 attempts to search for individual glyphs by
374 the 46 participants. There was one failed case, in which the user gave up the task after trying for
375 1.5 minutes. Among the 80 success cases, there were 71 cases where the users were able to
376 find the correct match within 1 minute. The longest time a user took to find a glyph was 3
377 minutes. We are not aware of any previous study similar to ours in the specific context of Maya
378 hieroglyphs, so this first result could be seen as a future baseline.



379

380 *Fig. 12 Query glyphs to be identified by general public users.*

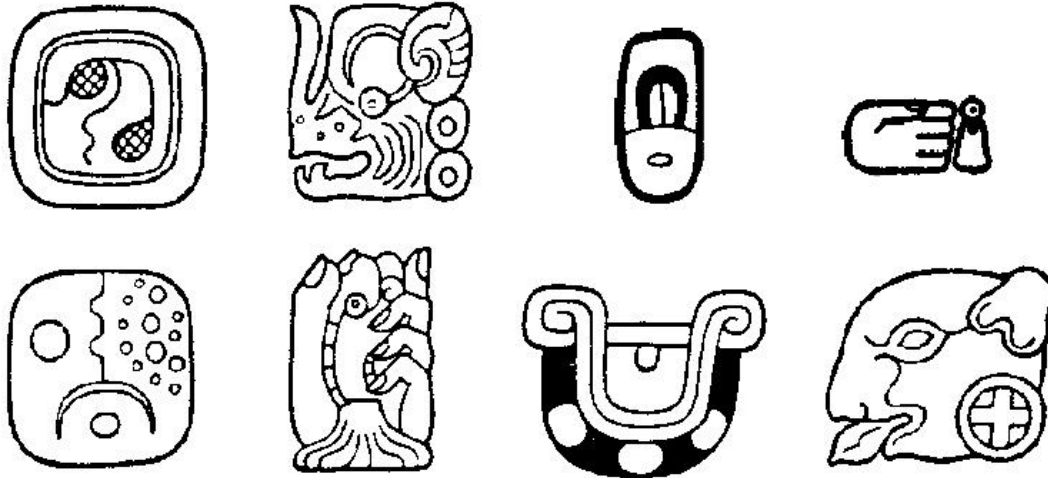
381

382 **Epigrapher scholar users.**

383 For the epigrapher scholars, we carefully picked 8 challenging glyphs which can be typically
384 difficult to identify without manually checking the catalog books (see Fig. 13). Epigraphers could
385 pick any glyph(s) from this list to work with. Scholars were advised to record the time they spent
386 to find each query glyph and report their experience.

387 The evaluation results show that the volunteer scholar who has less than 3 years' experience
388 was able to find all the 8 glyphs using our tool, among which 6 of them were identified within less
389 than 2 minutes, and the other 2 were identified in around 3 minutes. A second user also reported
390 the time he spent manually searching for the given glyph from the catalog book in comparison to

391 time spent using our tool. With the tool, this user was able to find 7 glyphs within 1 minute, which
392 is on average 1 minute shorter than his reported time to manually search the catalog. The third
393 user reported his searching experience on one glyph. It took the user 10 seconds to find it with
394 our tool, while he spent more than 5 minutes to find it manually in the catalog. Once again, these
395 times can be seen as a baseline for future comparison.



396

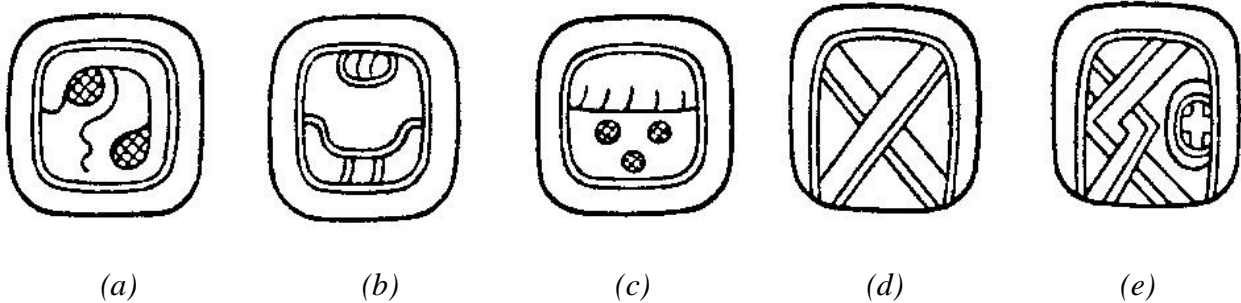
397 *Fig. 13 Query glyphs to be identified by the epigrapher scholar users.*

398 **3.2.2 Task II: Evaluating similar glyphs**

399 This task only targeted the epigrapher expert users. We invited participants to manually check
400 each similar glyph listed in the information panel for the 8 glyphs (Fig. 13) which were identified
401 in the previous task, to assess whether they are indeed sufficiently similar to the query glyph.
402 Additionally, participants were also asked to recommend any other visually similar glyphs that
403 were not listed by the tool. On average, there were 25 similar glyphs recommended for each of
404 the 8 query glyphs in our interface. This task aims to further evaluate our methodology to
405 measure the practical value of automatically computed glyph visual similarity.

406 For each query glyph, the expert participant carefully checked each of the recommended glyphs,
407 marked the ones that were not sufficiently similar to the query, and recommended additional
408 glyphs that were missing in the recommended list. This is a task that experts can perform well.
409 The scholar with less than three years' experience reported that on average 70% of the
410 recommended glyphs were considered to be visually similar to each of the 8 query glyphs.
411 However, the other two users could only agree on around 20% of the recommended glyphs. The
412 rest were not considered to be sufficiently similar due to various reasons, such as: the
413 recommended glyphs share similar contours to the query, but the contents are not sufficiently

414 similar (see Fig. 14 for examples); the glyphs share similar shape, but have different visual
415 references (such as a hand shape, a bird shape, etc.). Furthermore, the epigraphers typically
416 recommended 0-3 visually similar glyphs to each of the 8 query glyphs, which were not originally
417 included in the list.



420 *Fig. 14 Example query glyph (a), and negative examples (b-e) from the recommended visually*
421 *similar glyphs.*

422 **3.2.3 Task III: Applying glyph co-occurrence information**

423 This task is designed to evaluate our tool from the perspective of identifying problematic glyphs
424 within the context of glyph blocks, by using the glyph co-occurrence information provided in the
425 information panel. As introduced in section 2.3, context information (glyph co-occurrence) can be
426 used to assist the process of individual glyph identification, especially in cases where the query
427 glyph in a block is difficult to identify due to erosion, occlusion, etc. This task targeted only the
428 epigrapher scholar users.

429 For this task, we selected 3 partially damaged glyph blocks cropped from ancient Maya codices.
430 The task is to identify each individual glyph in these blocks. Glyph elements in these blocks are
431 ambiguous to be identified due to erosion. The participants were advised to make use of the
432 glyph co-occurrence information provided in the information panel to assist the identification
433 process.

434 In the results, participants commented that one glyph in one of the blocks was too damaged to
435 be recognized even with the help of the co-occurrence information; in the case of the other 2
436 blocks, the epigrapher participants stated that the glyph co-occurrence information provided in
437 our tool was clearly helpful to identify partially damaged glyphs.

438 **3.3 User feedback**

439 We designed questionnaires for the two user groups separately to further evaluate our interface.
440 Our objectives are threefold: first, to learn about the participants' background knowledge with

441 Maya glyphs; second, to find out whether it was overall a good experience to use our tool; finally,
442 to collect suggestions to improve the tool.

443 **3.3.1 General public user group**

444 From the feedback, 18 users stated that they had previously seen Maya glyphs from videos or
445 images, and had some brief knowledge about the topic; the rest of the users either had never
446 seen any glyphs before, or did not know about Maya writing before this experience. For all
447 users, this was the only tool they had ever encountered to explore and learn about ancient Maya
448 writing. Regarding user experience, users could select one of the five options, on a scale
449 ranging from terrible (1) to great (5). 26 users reported that it had been a great experience, and it
450 had inspired them to learn more about the ancient Maya culture; 18 users claimed that it had
451 been an interesting experience, they have learnt something from it; 2 users reported the
452 experience as being moderately interesting. Regarding the functionality of the tool, 42 users
453 stated that it was a useful tool and they would like to try it again; 4 users commented that it was
454 an interesting tool, but it could be improved. Last but not least, it is worth mentioning a few open
455 comments left by users in hand written form in the questionnaire. One user commented that it
456 would be interesting to apply such interface in museums for visitors to interactively explore the
457 Maya hieroglyphs during their visit. Another user suggested implementing a mobile version of
458 the tool. One participant coincidentally coming from the Yucatan region in Mexico, one of the
459 main Mayan regions, commented that it was a great experience for him to learn about this
460 research project and to explore Maya hieroglyphs through our tool.

461 **3.3.2 Epigrapher scholar user group**

462 From the feedback, our tool was the only one known to all three scholars for exploring Maya
463 hieroglyphs. It was rated as an interesting experience overall, very easy to use, and that it could
464 definitely be applied to assist the daily work of scholars. One participant also commented that
465 the interface could be further improved by incorporating an explicit searching functionality, where
466 users can locate a glyph in the graph by typing the corresponding Thompson glyph category
467 code to the search box.

468 **4. Conclusion**

469 We have introduced the HOOSC descriptor to be used in DH-related shape analysis tasks. We
470 discuss the effect of parameters on the performance of the descriptor in a glyph retrieval
471 framework. Experimental results on ancient Maya hieroglyph data from two different sources

472 (codex and monument) suggest that a larger spatial context with finer partitioning usually leads
473 to better results, while a smaller spatial context with location information is a good choice for
474 noisy/damaged data.

475 Additionally, we present a graph-based glyph visualization interface, which enables the
476 exploration and analysis of hieroglyphs. The HOOSC descriptor is used to represent the shape
477 of glyph images, based on which the pairwise glyph similarity scores are computed to define
478 edge weights of the graph.

479 From the evaluation we conducted with the users, the interface provides an efficient way to
480 browse and explore hieroglyphs. Additionally, Task I and Task II confirmed the effectiveness of
481 the HOOSC descriptor to represent historical Maya glyphs. Results from Task III suggested that
482 the glyph context information provided in our interface can be used to identify problematic glyphs
483 within a block.

484 The code for HOOSC is available so DH researchers can test the descriptor for their own tasks.
485 Finally, the browsing interface is also publicly available and will be used for further study with the
486 general public and expert users.

487 Acknowledgement

488 We thank Edgar Roman-Rangel for co-inventing the HOOSC algorithm and providing the original
489 code. We also thank Guido Krempel, and Jakub Spotak for producing some of the codical data
490 used in this paper. Finally, we thank the Swiss National Science Foundation (SNSF) and the
491 German Research Foundation (DFG) for their support through the MAAYA project.

492

493 References

494 **Belongie, S., Malik, J., and Puzicha, J.** (2002). Shape Matching and Object Recognition using
495 Shape Contexts. *PAMI*. PP. 509-522.

496 **Bostock M., Ogievetsky V., Heer J.** (2011). D3: Data-Driven Documents. *IEEE Trans. Vis.*
497 *Comput. Graph.* pp. 2301-2309.

498 **Dalal, N., and Triggs, B. (2005).** Histogram of Oriented Gradients for Human Detection. *In*
499 *CVPR*. pp. 886-893.

500 **Eitz, M., Richter, R., Boubekeur, T., Hildebrand, K., and Alexa, M.** (2012). Sketch-based
501 shape retrieval. *ACM Transactions on Graphics*. pp. 31:1-31:10

502 **Fischer, A., Bunke, H., Naji, N., Savoy, J., Baechler, M., and Ingold, R.** (2012). The HisDoc
503 Project. Automatic Analysis, Recognition, and Retrieval of Handwritten Historical Documents for
504 Digital Libraries. *InterNational and InterDisciplinary Aspects of Scholarly Editing*.

505 **Franken, M., and Gemert, J. C.** (2013). Automatic Egyptian Hieroglyph Recognition by
506 Retrieving Images as Texts. *ACM MM*, pp. 765-768.

507 **Hu, R., Odobez, J. M., Gatica-Perez, D.** (2016). Assessing a Shape Descriptor for Analysis of
508 Mesoamerican Hieroglyphics: A View Towards Practice in Digital Humanities. *Digital*
509 *Humanities Conference*.

510 **Hu, R., Can, G., Pallan, C. G., Krempel, G., Spotak, J., Vail, G., Marchand-Maillet, S.,**
511 **Odobez, J. M., and Gatica-Perez, D.** (2015). Multimedia Analysis and Access of Ancient Maya
512 Epigraphy: Tools to support scholars on Maya hieroglyphics. *IEEE Signal Processing Magazine*.
513 pp. 75-84.

514 **Montgomery, J., and Helmke, C.** (2007). Dictionary of Maya Hieroglyphs,
515 <http://www.famsi.org/mayawriting/dictionary/montgomery/>.

516 **Roman-Rangel, E.** (2012). Statistical Shape Descriptors for Ancient Maya Hieroglyphs Analysis.
517 *PhD thesis, EPFL*.

518 **Roman-Rangel, E., Pallan, C. G., Odobez, J. M., and Gatica-Perez, D.** (2011). Analyzing
519 Ancient Maya Glyph Collections with Contextual Shape Descriptors. *IJCV*. pp. 101-117.

520 **Stone, A.J. and Zender, M.** (2011). Reading Maya Art: A Hieroglyphic Guide to Ancient Maya
521 Painting and Sculpture. *Thames & Hudson Limited Publisher*.

522 **Thompson, J. E. S.** (1962). a Catalog of Maya Hieroglyphs. *University of Oklahoma Press*.

523 **Vail, G., and Hernández, C.** (2013). The Maya Codices Database, Version 4.1. A website and
524 database available at <http://www.mayacodices.org/>.